In-situ aircraft observations of the 2000 Mt. Hekla volcanic cloud: Composition and chemical evolution in the Arctic lower stratosphere

D.E. Hunton[a],*, A.A. Viggiano[a], T.M. Miller[a], J.O. Ballenthin[a],
J.M. Reeves[b], J.C. Wilson[b], Shan-Hu Lee[b], B.E. Anderson[c],
W.H. Brune[d], H. Harder[d], J.B. Simpas[d], N. Oskarsson[e]

[a]Air Force Research Laboratory, Space Vehicles Directorate, Hanscom AFB, MA 01731, United States
[b]Department of Engineering, University of Denver, Denver, CO 80208, United States
[c]NASA Langley Research Center, Hampton, VA 23681, United States
[d]Department of Meteorology, Pennsylvania State University, State College, PA 16802, United States
[e]Nordic Volcanological Institute, Reykjavik, Iceland

Abstract

An instrumented NASA aircraft made comprehensive, in-situ measurements of trace gas concentrations and aerosol properties while flying through the eruptive cloud from Mt. Hekla in February and March, 2000. The data reveal novel aspects of the properties and evolution of the volcanic cloud in the lower arctic stratosphere. Thirty-five hours after the initial, sub-Plinian explosion on February 26, 2000, the aircraft intersected the cloud at an altitude of 11.3 km. SO_2 concentrations in the cloud exceeded 1 ppmv, but no H_2S was observed. Large HF concentrations of ~50 ppbv were nearly equal to the HCl concentration, the same ratio of halogen species adsorbed on fallen ash. Although reactive nitrogen species are rarely detected in volcanic clouds, significant HNO_3 concentrations of 3 ppbv above background were measured. A bimodal aerosol size distribution with total number densities exceeding 8000 particles/cm^3 and total aerosol volume of 65 $\mu m^3/cm^3$ was observed. Approximately 1/3 of the fine aerosol particles were non-volatile (volcanic ash) and the remaining 2/3 were volatile (sulfate aerosol and ice). The volcanic cloud was highly structured with clearly delineated boundaries. In the 18-day period following the initial eruption, increases in SO_2, sulfate aerosol, HCl, and HF volume mixing ratios were again detected. Analysis of the partitioning of sulfur between the gas and aerosol phases in these later cloud encounters shows that the rate of SO_2 oxidation to sulfuric acid was broadly consistent with changing OH concentrations at the time of the vernal equinox.
Published by Elsevier B.V.

* Corresponding author.
  E-mail address: donald.hunton@hanscom.af.mil (D.E. Hunton).

1. Introduction

NASA's DC-8 flying laboratory flew directly through the eruptive cloud from Mt. Hekla, a volcano near the southern shore of Iceland, on February 28, 2000. The instruments aboard the research aircraft obtained a comprehensive portrait of the trace gas composition, aerosol properties, and meteorological conditions in the volcano cloud. On additional science flights in March, made as part of the first SAGE-III Ozone Loss and Validation Experiment (SOLVE) campaign (Newman et al., 2002), the aircraft again encountered evidence of the cloud. Aircraft encounters with volcanic clouds are rare. These serendipitous SOLVE data therefore provide a unique opportunity to study the time evolution of a volcanic cloud in the Upper Troposphere/Lower Stratosphere (UT/LS).

Mt. Hekla began erupting at 18:18 UT on 26 February 2000. The volcanic cloud formed during its short, sub-Plinian, explosive phase carried ash, trace gases, ice, and sulfate aerosol into the lower strato-sphere. The total ozone mapping spectrometer (TOMS) instrument (Krotkov et al., 1997) aboard the Earth Probe Satellite detected the Hekla SO_2 cloud (Fig. 1) at 11:54 UT on 27 February, about 17.5 h after the eruption onset (Krueger et al., 2000). A comprehensive analysis of the TOMS data and other satellite images of the eruption has been given by Rose et al. (2003). Following the initial injection of ash and gas into the stratosphere, the volcano continued to release outgassing products into the atmosphere through Strombolian explosions and buoyant rising of hot air above lava flows until March 8.

Volcanoes are a major source of sulfur dioxide (SO_2) in the atmosphere (Bandy et al., 1982; Castle-man et al., 1974; Hobbs et al., 1981; Krotkov et al., 1997; Mankin et al., 1992). Chemical oxidation of SO_2 by hydroxyl radical (OH) produces gas phase sulfuric acid (H_2SO_4) that, in turn, undergoes nucle-ation to form sulfate aerosol particles (Turco et al., 1982; Wayne, 1991). Increased atmospheric aerosol can have significant effects on the earth's atmosphere
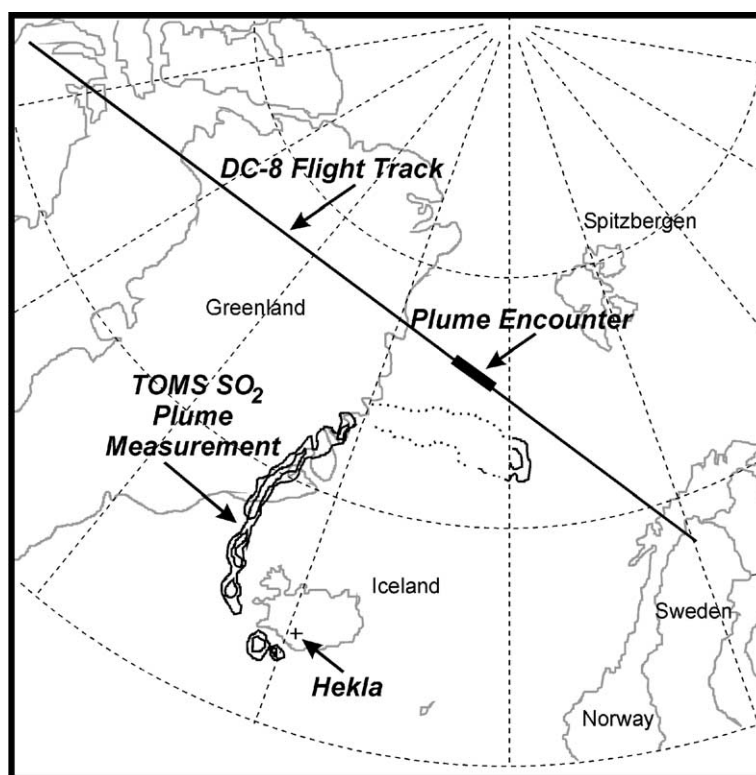

Fig. 1. Map of the DC-8's great circle flight track from Edwards Air Force Base, California to Kiruna, Sweden.

and climate (Grainger and Highwood, 2003; Robock, 2000; Solomon, 1999). In this paper, we focus first on the composition of the plume on February 28th and then on the conversion of SO_2 to sulfate aerosol using trace gas composition data from the chemical ionization mass spectrometer (CIMS), OH concentrations from the airborne tropospheric hydrogen oxides sensor (ATHOS), and aerosol size distributions and volumes from two suites of aerosol sampling instruments.

2. Instrumentation

The first SAGE-III Ozone Loss and Validation Experiment (SOLVE-I) was conducted from Kiruna, Sweden between December, 1999, and March, 2000 (Newman et al., 2002). Coordinated flights of NASA's DC-8 and ER-2, other aircraft, and balloon payloads were conducted in the high latitude region roughly between Sweden and the North Pole and between Greenland and Novaya Zemlya.

The DC-8 flight path for the transit between California and Sweden on February 28 is plotted in Fig. 1 along with the outline of the SO_2 cloud from Hekla detected by the TOMS instrument 17 h earlier. The aircraft took off from Dryden Research Center at 21:07 UT on February 27th. It intercepted the Hekla cloud at an altitude of 37,000′ (11.3 km) between 5:08 and 5:18 UT on February 28, 35 h after the start of the eruption. The position of the plane at these times is shown as the thick line segment along the flight path. The Total Ozone Mapping Spectrometer (TOMS) instrument aboard the Earth Watch Satellite was favorably positioned once per day to detect the Hekla SO_2 plume. The SO_2 retrieval image from February 27th, taken at 11:54 UT or about 17.5 h after the eruption onset, clearly shows a well-defined SO_2 plume curling clockwise away from Iceland to the southwest and then around to the north and east. Fig. 1 is based on the February 27th TOMS retrieval and shows approximate contours of the plume. The dotted lines estimate the position of the plume in darkness beyond the solar terminator where the TOMS instrument cannot collect data. The image obtained one day later shows the remnants of the plume far to the east of Iceland over northern Russia and Finland. The plume was not seen again in later TOMS images.

The DC-8 payload for the SOLVE mission consisted of 17 scientific instruments or suites of instruments (Newman et al., 2002). The chemical ionization mass spectrometer (CIMS) from the Air Force Research Laboratory (Ballenthin et al., 2003; Hunton et al., 2000; Miller et al., 2000; Talbot et al., 1999; Viggiano and Hunton, 1999), one of the in-situ trace gas instruments, was optimized to measure the mixing ratios of HNO_3, SO_2, and HCN. The instrument was also sensitive to H_2SO_4, HCl, HF, and H_2S, though the concentrations of these gases were obtained at lower time resolutions.

Aerosol size and number measurements were made by the University of Denver focused cavity aerosol spectrometer (FCAS II) (Jonsson et al., 1995) and nuclei-mode aerosol size spectrometer (N-MASS) (Brock et al., 2000). The N-MASS detected particles in the diameter range 4 to 100 nm, while the FCAS II covered 90 to 2000 nm. Corrections were made for diffusion loss, instrument efficiencies, and departures from isokinetic sampling at the inlet. The combined measurements were then inverted to obtain the full aerosol size distribution from 4 to 2000 nm. The total volume of aerosol particles was calculated by integrating the size distribution. Additional aerosol properties, including the volatile and nonvolatile fractions of aerosol concentrations, and the concentrations of larger particles were measured by the NASA Langley particle measurement system (PMS) (Anderson et al., 1998a,b).

Gas phase OH concentrations were obtained with the Pennsylvania State University Airborne Tropospheric Hydrogen Oxides Sensor (ATHOS) (Brune et al., 1998, 1995). ATHOS used laser-induced fluorescence to detect OH concentrations as low as 0.015 pptv at a sampling rate of 5 Hz. All of the OH concentrations observed during the March SOLVE deployment are plotted against solar zenith angle in Fig. 2. The quadratic least squares fit to these data is also shown. Agreement of the observed [OH] values with the predictions of a one-dimensional photochemical model was found to be acceptable throughout the range of measurements. The model overestimated the measurements by approximately 10% at lower SZA values and by about 40% at SZA values near 90 degrees. When the [OH] data were separated into measurements taken inside the volcanic clouds and outside, no significant difference in the
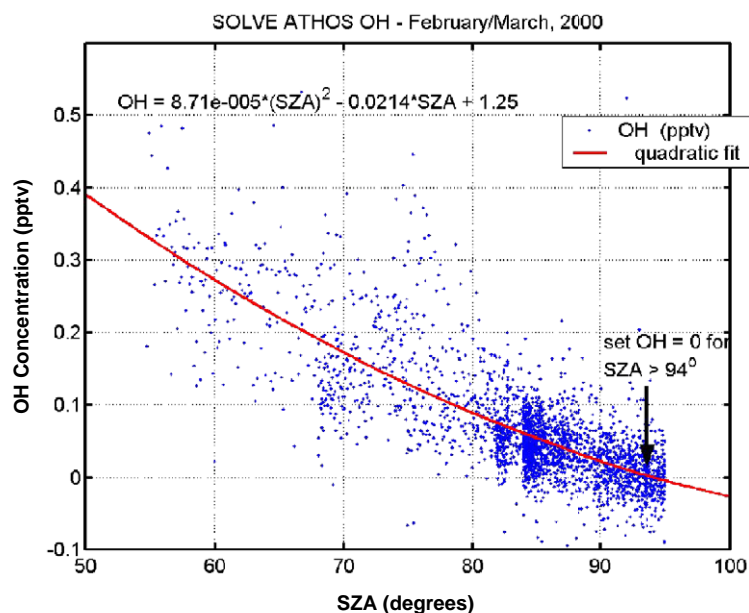
Fig. 2. Variation in measured OH concentration in parts per trillion by volume (pptv) vs. solar zenith angle. The quadratic least squares fit used to calculate [OH] from SZA along the back trajectories from plume intercept points is also plotted.

least squares fit was observed. This observation reflects the fact that the SO_2+OH reaction is not a significant additional loss mechanism for OH at the concentrations of SO_2 encountered.

3. Initial cloud crossing—February 28

Trace gas concentrations and aerosol properties from the 28 February cloud crossing are plotted in Fig. 3. The top panel shows CIMS measurements of SO_2 and H_2SO_4 volume mixing ratios (VMRs), while the middle panel plots HCl, HF, and HNO_3 VMRs. The bottom panel shows aerosol number densities in the 12–1000 nm diameter range from the Langley instrument suite. The variations in the trace gas concentrations and the aerosol properties with horizontal distance across the volcanic cloud are well correlated with each other and show very detailed structure. Gradients in concentrations are large; the SO_2 concentration, for example, changed by 1 ppmv in horizontal distances of approximately 2 km at the edge of the cloud.

SO_2 VMRs in this region of the cloud exceeded 1 part per million by volume (ppmv). In contrast, the SO_2 concentrations measured throughout all of

December 1999 and January 2000 were less than 100 parts per trillion by volume (pptv) and showed little or no spatial variation. These measurements provided "ground" truth for validation of the satellite analyses, which were in excellent agreement (Rose et al., 2003). The concentration of gas-phase H_2SO_4 was less than 0.04% of the SO_2 VMR. Gas phase H_2SO_4 has been detected previously in association with volcanic activity (Arnold and Bührke, 1983; Qiu and Arnold, 1982), though not in a discrete cloud. Recent calculations of the gas-phase H_2SO_4 concentration for the conditions of the Hekla encounters were performed using a detailed, one-dimensional, microphysical model (Klein et al., 2000). The calculated H_2SO_4 concentrations were lower than the observations by approximately an order of magnitude, indicating that some small sulfate aerosol particles may have been drawn into the CIMS instrument and evaporated in the heated sampling tube. The model also showed that the time dependence of the gas phase H_2SO_4 concentration tracked solar zenith angle and [OH] accurately, indicating that the lifetime of gas phase H_2SO_4 with respect to condensation into aerosol was on the order of hours or less. We view the measured H_2SO_4 concentrations as upper limits to the true gas phase concentrations, and conclude that
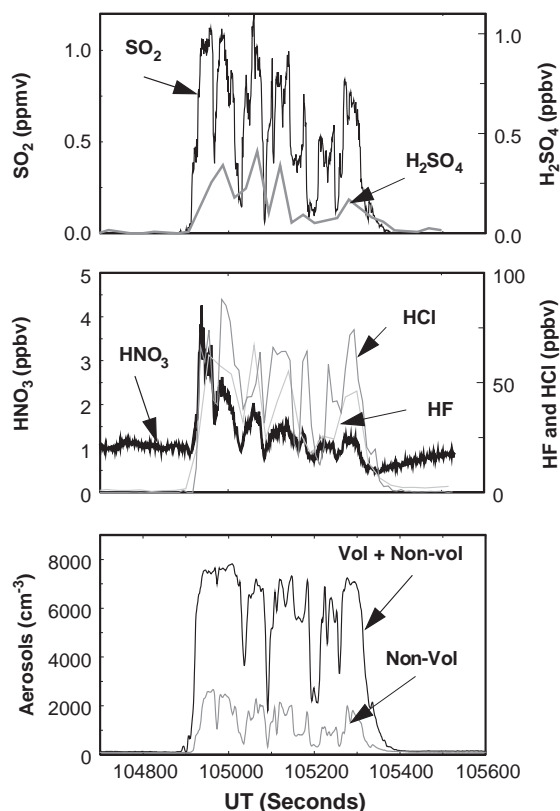
Fig. 3. In-situ measurement of plume properties between 5:08 and 5:18 UT on 28 February, 35 h after the eruption began. The aircraft was at 11.3 km altitude off the east coast of Greenland (Fig. 1). The time scale for each panel is seconds in Universal Time (UT) counting from 0:00 h on 27 February, the day the flight began.

that gas phase concentration was negligible in comparison with the mass of H_2SO_4 contained in the aerosol phase.

Two halogen species, hydrogen chloride (HCl) and hydrogen fluoride (HF), were observed in the cloud at concentrations of approximately 50 parts per billion by volume (ppbv). Explosive volcanic eruptions can inject substantial quantities of HCl into the stratosphere (Mankin and Coffey, 1984; Mankin et al., 1992), though tropospheric scavenging can remove much of the gas from the cloud before it reaches the stratosphere (Tabazadeh and Turco, 1993). The HCl/SO_2 ratio in the February 28 cloud was 0.07. Although this is lower than the ratios of near unity detected at the craters of some volcanoes or in the troposphere (Francis et al., 1995; Horrocks et al., 1999; Oppenheimer et al., 1998), the extent of

tropospheric scavenging of HCl in Hekla's case cannot be assessed because the initial HCl/SO_2 ratio is not known.

Magmas from Icelandic volcanoes are fluorine rich. The F/Cl ratio of scavenged halogens in ash collected after the 1970 Mt. Hekla eruption was close to 0.8 (Oskarsson, 1980). Identical ratios have been measured at The Nordic Volcanological Center (NORDVULK), Reykjavik, Iceland, in ash following the 1980, 1991, and 2000 eruptions. The February 28 cloud shows the same fluorine signature: the average HF/HCl VMR ratio in the cloud was 0.87, essentially the same value as in the ash. This result may indicate that the scavenging rates for the two halogen species are very similar.

Nitrogen oxides (NO_x=NO and NO_2) and other reactive nitrogen species (collectively called NO_y and including NO_x, N_2O_5, HNO_2, HNO_3, $ClONO_2$, PAN and others) are not commonly detected in volcanic plumes, and we are aware of only a few previous observations. An increase in nitric acid (HNO_3) concentration was noted in conjunction with an aerosol layer produced by the El Chichón eruption (Qiu and Arnold, 1988). NO and NO_2 have both been detected at Mt. St. Helens (Bandy et al., 1982; Hobbs et al., 1981). HNO_3 has recently been reported in persistent plumes at ground level from four volcanoes (Mather et al., 2004). However, the data from the present Hekla encounter represent the first time that HNO_3 has conclusively been detected in an explosive volcanic cloud in the UT/LS. As shown in the center panel of Fig. 3, the HNO_3 VMR reached a peak of 3 ppbv above the background. This measurement was corroborated by another instrument aboard the aircraft [Koike, private communication, 2000]. The source of the HNO_3 is not known although oxidation of the ammonia that is an outgassing product of Hekla lavas (Oskarsson, 1981) may play a role. The variation in HNO_3 as a function of position across the cloud, peaking more strongly on the western edge, is different from the other gases and the smaller aerosol particles. We note that the variation in the concentration of particles larger than 2 μm with position in the cloud is similar to that of the HNO_3, although the tie between the larger particles and the HNO_3 is not known.

The CIMS did not detect changes in the hydrogen cyanide (HCN) or hydrogen disulfide (H_2S) signals in

the Hekla cloud. The instrument is sensitive to these gases and upper limits to the concentrations could be determined. The HCN VMR was less than 100 pptv and the H_2S VMR was less than 15 ppbv. The upper limit implies that the H_2S/SO_2 ratio must have been less than 0.015. The small H_2S/SO_2 ratio and the possible conversion of NH_4 to HNO_3 are both consistent with the highly oxidizing nature of volcanic plumes.

In the aerosol measurements shown in the lower panel of Fig. 3, both the unheated inlet (volatile plus non-volatile) and the heated inlet (non-volatile) channels are shown. The difference between the two signals is the volatile portion of the aerosol and likely comprised ice and sulfate. The non-volatile portion was most likely due to volcanic ash. The spatial distribution of aerosol particles was the same as for the SO_2 and the other trace gases. There is no evidence, therefore, of horizontal separation between the gas and particle phases of the cloud. The size distribution of the aerosol particles detected in the plume was bimodal with peaks at 0.07 μm and at 0.36 μm diameter. Total aerosol number concentration peaked at 7500 cm^{-3}, aerosol volume equaled 65 $μm^3/cm^3$ in the densest position in the cloud, the surface area reached 950 $μm^2/cm^3$, and the ratio of volatile aerosol (sulfate and ice) to non-volatile (ash) was approximately 2:1.

4. Subsequent cloud intercepts—March 5–15

Throughout most of the SOLVE DC-8 missions in March, 2000, the CIMS detected many discrete spikes in SO_2 concentration between 500 pptv and 15 ppbv that were consistently accompanied by increases in aerosol number and volume concentrations. These measurements were taken at flight altitudes between 10 and 12.5 km. Data from one of the largest events are shown in Fig. 4. The congruence between the measurements is excellent. Again, there is no horizontal separation between the gas and aerosol phases. Many similar cloud encounters were seen on March 5, 8, 9, 13, and 15. Table 1 summarizes the trace gas and aerosol properties observed in the largest encounter on each day. In the two cases in March when the SO_2 concentration was the greatest, trace amounts of HCl and HF were also detected. Because the halogen species were observed in coincidence with the SO_2 and aerosols and because there is no other known
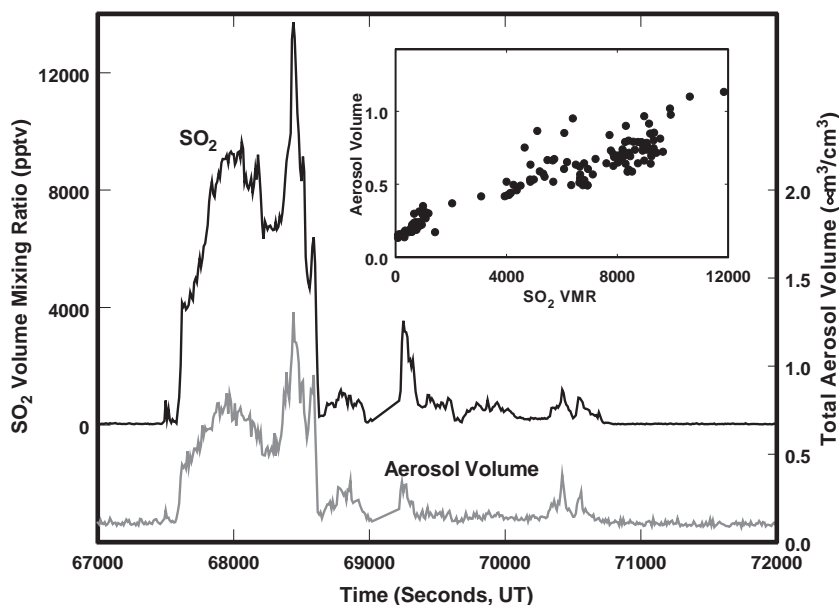

Fig. 4. Correlated measurements of SO_2 concentration from the CIMS and total aerosol volume from the aerosol size distributions derived from the NMASS/FCAS data. The data are from a 1.4 h period of the March 13 SOLVE science flight at an altitude of 11.3 km. The inset graph plots aerosol volume against SO_2 concentration with the same units as the main graph for the large peak between 67,500 and 68,700 s.

Table 1
Hekla plume composition observations[a]

	Feb 28	Mar 5	Mar 8	Mar 9	Mar 13	Mar 15
Days after eruption	1.45	7.77	10.77	11.94	15.94	17.52
SO_2 (ppb)	895	0.12	0.16	3.45	10.6	1.50
H_2SO_4 (ppb)	0.31	–	–	0.1	0.08	–
HCl (ppb)	60.2	–	–	0.1	0.50	–
HF (ppb)	57.2	–	–	0.3	<0.2	–
HNO_3 (ppb)	3.2	–	–	–	–	–
Aerosol[b] number density (cm^{-3})	7430	64	429	6033	3073	1068
Aerosol[b] VMR ($\mu m^3/cm^3$)	85.8	<0.05	<0.05	0.41	1.50	0.46

[a] Peak values of 60-s averages above background.
[b] Diameter range: 4 nm to 2 μm.

source of lower stratospheric SO_2 that could have produced the observed spikes in concentration, we conclude that all the SO_2 and aerosol spikes were produced by volcanic activity from Mt. Hekla.

As noted earlier, Hekla's activity in 2000 was not limited to the initial explosive event on February 26 that injected the volcanic cloud directly into the stratosphere. Lava fountains and intermittent explosions continued with varying intensity until March 3. Lava flows did not abate until March 8. Large lava flows and fountains can lead to complete degassing of the flowing silicate melt. The volatile species can then rise into the atmosphere by buoyancy or explosive force. Thus, it is possible that some of the cloud crossings observed in March may have originated with the later activity rather than from the original February 26 injection.

To differentiate between a stratospheric or lower tropospheric origin of the SO_2 features observed in March, we have examined carbon monoxide–ozone correlations for the February and March, 2000, flights. The relationship between these two trace gases can be used to identify regions of recent mixing between the troposphere and lower stratosphere (Fischer et al., 2000; Hipskind et al., 1987; Hoor et al., 2002). Stratospheric air that has not been influenced by tropospheric mixing in the last several months has low equilibrium concentrations of CO near 15–20 ppbv and variable, high, concentrations of ozone. On tracer–tracer scatter plots, these air masses appear as a nearly vertical stratospheric branch. Tropospheric air, conversely, has low ozone concentrations and

variable, higher CO concentrations. These air masses give rise to a horizontal, tropospheric branch. Recent mixing, on time scales of days to weeks, produces data points along mixing lines with slopes intermediate between the two other branches.

The CO–O_3 scatter plots from March 2000 shown in Fig. 5 are similar to those from March, 1997 (Hoor et al., 2002). All show stratospheric and tropospheric branches to some extent, and all indicate that there is a mixing layer in the lower stratosphere. The subsets of these data obtained within the volcanic cloud are highlighted in the plots. On February 28, the cloud air masses depart significantly from the undisturbed atmosphere because of a combination of CO production by the volcano, chemical depletion of ozone, and entrainment of tropospheric air in the cloud. On the other 3 days, the SO_2 cloud air masses lie exactly along the ambient CO–O_3 curve. Dilution of the volcanic gases by a factor of 100 to 1000 compared to the February 28 intercept makes the CO and O_3 concentrations in the cloud remnants indistinguishable from the background. On March 9 and 13, the intercepts with the SO_2–aerosol features were entirely within the stratospheric branch. On March 5 and 8, the SO_2 events were detected at the transition point between the stratospheric branch and the mixing region. On March 15, the SO_2 events extended well into the mixing region, but not to the tropospheric branch. This may be an indication of downward transport from the lower stratosphere. We conclude that the SO_2–aerosol spikes detected on the DC-8 in March are not consistent with buoyant lofting of degassed material from the later volcanic activity because they were detected well within the unmixed stratosphere, not within the lower levels of the mixing layer. They must, therefore, be remnants from the initial explosive injection of volcanic gases into the stratosphere on February 26.

Because the SO_2 was injected into the stratosphere in a short period of only a few hours, the data from the March cloud encounters can be used to investigate the kinetics of SO_2 oxidation in the atmosphere. We cannot follow the global decrease of volcanic SO_2 because individual measurements of the SO_2 VMR reflect only what portion of the volcanic cloud was observed, not the total amount of the gas remaining in the atmosphere. However, with a single cell (or zero-dimensional) model of the kinetics, the rate of SO_2
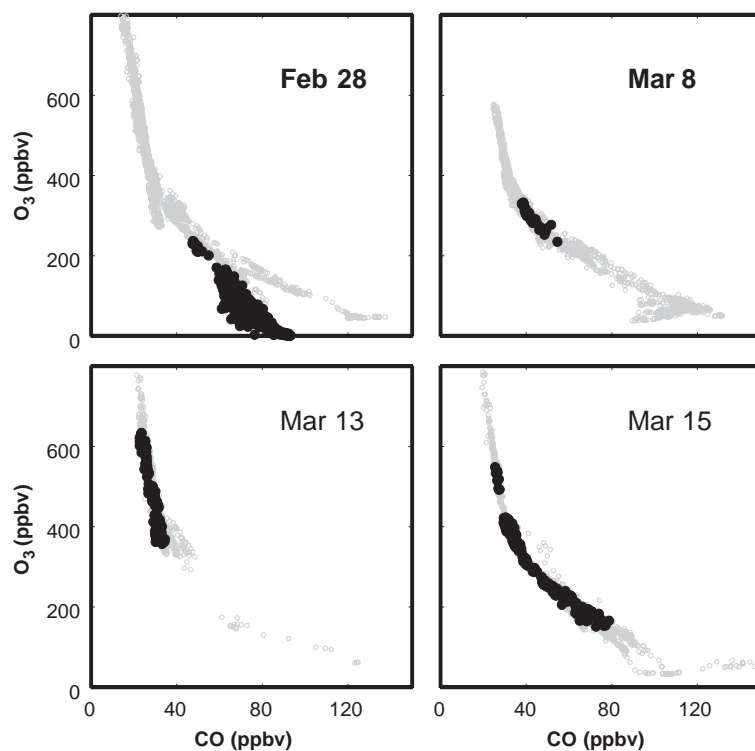
Fig. 5. Four representative CO–O_3 scatter plots for flight days in February and March, 2000. In each panel, the data for the entire flight are plotted in gray while the data obtained in the SO_2–aerosol cloud intercepts are highlighted in black.

conversion to sulfate aerosol within each plume air parcel is governed by the same kinetics as the total mass of SO_2. The amount of conversion is reflected in the ratio of the amount of sulfur that appears as sulfate in each plume crossing to the amount that remains as gas phase SO_2. A single cell model is appropriate to a first approximation. The particles detected in March are similar in size to the stratospheric accumulation mode aerosol and are too small to settle appreciably in the time between the eruption and the cloud encounters. Further, there is no observed horizontal separation between the gas and the aerosol particles. The gas phase SO_2 and the aerosol particles move together and become diluted by the same amount.

For each separate volcanic cloud fly-through, the mass ratio of aerosol phase sulfur to gas phase sulfur was calculated from the slope of the scatter plot of SO_2 concentration against aerosol volume (Fig. 4, inset). Aerosol volume was converted to the mass of S in the aerosol phase using an average density for the sulfate aerosol particles of 1.82 g/cm^3 and an average

bulk composition of 96% H_2SO_4 by weight (the aerosols are dehydrated in the sampling process). The mixing ratio of gas phase SO_2 was converted to a mass of S per cm^3 using the measured temperature and pressure in the plumes. The Langley aerosol instruments showed that there was no non-volatile fraction of particles in any of these plume crossings. Instrumental uncertainties are estimated to be ±30% in aerosol volume, ±30% in SO_2 mixing ratios, and ±40% in OH concentration. The measured values of the sulfur mass ratio are plotted in Fig. 6 as a function of time in days after the eruption. Qualitatively, the measured mass ratio increases with time reflecting the gradual conversion of SO_2 to sulfate.

H_2SO_4 is formed from SO_2 in the atmosphere in a series of well-studied reactions, starting with the rate-determining oxidation of SO_2 by OH (Turco et al., 1982). Since the reaction is pseudo-first order, the overall SO_2 lifetime (τ) can be related to the average concentration of OH by $1/\tau = k_{eff}$ [OH], where k_{eff} is the effective two-body rate constant for the reaction of
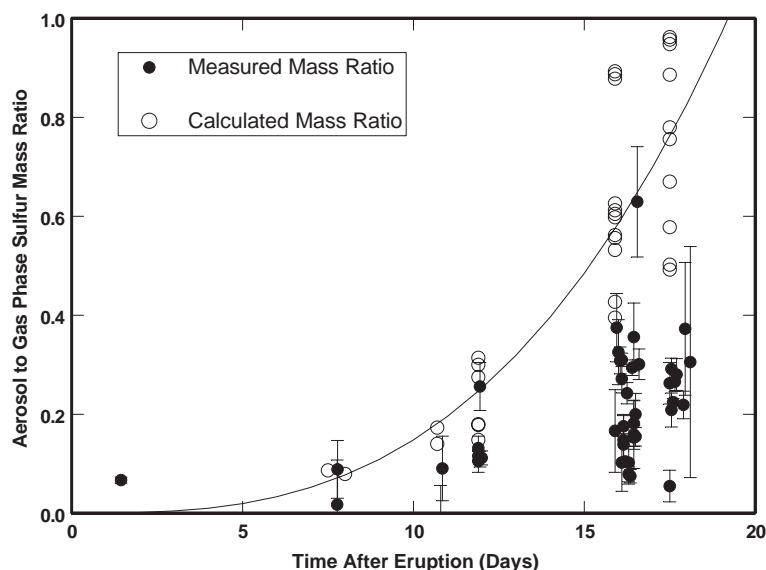
Fig. 6. The ratio of the mass of sulfur in the form of aerosol-phase H_2SO_4 to the mass of sulfur as gas-phase SO_2 as a function of time after the eruption. The solid circles with error bars are measurements from individual plume crossings. The open circles show the results of calculating the amount of SO_2 oxidation by integrating OH concentrations along isentropic back trajectories from plume intercept locations. The solid line is a fit through the calculated points to guide the eye. In several places, the points have been spread out horizontally for clarity.

SO_2 with OH and [OH] is the average number density of OH (Read et al., 1993; Rose et al., 2003). However, the SO_2 concentrations and aerosol properties were measured at high latitude just before the vernal equinox when the daily solar exposure and the concentrations of OH were changing rapidly. A single average OH and a single lifetime value do not adequately represent the conditions.

We have modeled the conversion from gas phase SO_2 to sulfate aerosol by integrating the instantaneous SO_2+OH reaction rate along isentropic back trajectories (Lait, 2002; Schoeberl and Sparling, 1994) from the cloud intercept positions. The only parameters that enter into the calculation are the OH concentration and the reaction rate. The concentration of OH depends strongly on the solar zenith angle (SZA) (Hanisco et al., 2001). A quadratic fit to the measured OH values obtained during the February/March SOLVE deployment varies from 0 pptv at SZA >94 degrees to ~0.33 pptv at SZA=55 degrees (Fig. 2). This fit was used to calculate [OH] from the SZA at each position along the back trajectories. For the average conditions at the plume intercept points (T=210 K and P=226 mbar), k_{eff}=8.9×10^{-13} cm^3 s^{-1} (DeMore et al., 1997). Small variations in atmospheric

conditions only change the rate slightly. The model calculation was done with a 1/25 day time step and was initialized at the time the SO_2-containing air parcel was first injected into the lower stratosphere. Uncertainties in the modeling are estimated to be ±30% in the assumption that the SO_2+OH reaction rate does not vary along the trajectory, ±10% in the assumption that [OH] does not depend on pressure or temperature, and ±75% in the calculation of [OH] from solar zenith angle along the 10–15 day back trajectories. The instrumental and calculation errors combine to give a total ±100% uncertainty in comparing calculated to measured mass ratios.

The model calculations of the sulfur mass ratio and the measured mass ratios (Fig. 6) both show the same qualitative behavior of an onset a few days after the eruption and then a marked increase as the solar exposure increases. Quantitatively, however, the model ratios are about a factor of three higher than the measurements. We have not identified any clear sources of a systematic error. For example, the OH concentrations inside the cloud crossings are not measurably lower than the ambient values. Also, SO_2 uptake on volcanic ice particles is important in early phases of an eruption, but analysis of satellite images of

the Hekla eruption showed that this sulfur was re-released into the gas phase several days after the eruption (Rose et al., 2003). SO_2 uptake is not known to occur on sulfate aerosols in the stratosphere. Finally, the trace gas correlation plots show that the SO_2 clouds detected in March were not due to later activity of the volcano. The most likely remaining possibility are errors in the trajectory analyses that could have predicted excursions of the volcanic air masses too far to the south. Because the disagreement is nearly consistent with the combined random errors in the model and measurements, we conclude that the measurements and the model agree within the limitations of the modeling approach. It is clear that the lifetime of SO_2 in the arctic winter stratosphere must be significantly longer than in other regions of the atmosphere because the OH concentrations are negligible.

5. Conclusions

The NASA DC-8 collected a unique, serendipitous data set on atmospheric effects of volcanic activity during its flights in February and March 2000. The initial analysis of these data presented here validates the kinetics of SO_2 oxidation. The trace gas portrait of the initial, explosive plume also reveals novel features of the Hekla emissions, including the presence of nitric acid and the similarity of the halogen signature in the cloud to that observed in ash fallout. Further analysis of the data will prove to be a powerful tool for exploring plume-atmosphere transport and mixing, gas-to-particle conversion, trace gas chemistry, satellite ground truth analysis, and other aspects of volcano–atmosphere interactions.

References

Anderson, B.E., Cofer, W.R., Bagwell, D.R., Barrick, J.W., Hudgins, C.H., Brunke, K.E., 1998a. Airborne observations of aircraft aerosol emissions: I. Total nonvolatile particle emission indices. Geophys. Res. Lett. 25 (10), 1689–1692.

Anderson, B.E., Cofer, W.R., Barrick, J.D., Bagwell, D.R., Hudgins, C.H., 1998b. Airborne observations of aircraft aerosol emissions: II. Factors controlling volatile particle production. Geophys. Res. Lett. 25 (10), 1693–1696.

Arnold, F., Bührke, T., 1983. New H_2SO_4 and HNO_3 vapour measurements in the stratosphere—evidence for a volcanic influence. Nature 301 (5898), 293–295.

Ballenthin, J.O., Thorn, W.F., Miller, T.M., Viggiano, A.A., Hunton, D.E., Koike, M., Kondo, Y., Takegawa, N., Irie, H., Ikeda, H., 2003. In-situ HNO_3 to NO_y instrument comparison during SOLVE. J. Geophys. Res. 108 (D6) (ACH 7-1-7-11, 4188 doi:10.1029/2002JD002136).

Bandy, A.R., Maroulis, P.J., Wilner, L.A., Torres, A.L., 1982. Estimates of the fluxes of NO, SO_2, H_2S, CS_2 and OCS from Mt. St. Helens deduced from in situ plume concentration measurements. Geophys. Res. Lett. 9 (9), 1097–1100.

Brock, C.A., Schröder, F., Kärcher, B., Petzold, A., Busen, R., Fiebig, M., 2000. Ultrafine particle size distributions measured in aircraft exhaust plume. J. Geophys. Res. 105, 26555–26567.

Brune, W.H., Stevens, P.S., Mather, J.H., 1995. Measuring OH and HO_2 in the troposphere by laser-induced fluorescence at low pressure. J. Atmos. Sci. 52, 3328–3336.

Brune, W.H., Faloona, I.C., Tan, D., Weinheimer, A.J., Campos, T., Ridley, B.A., Vay, S.A., Collins, J.E., Sachse, G.W., Jaegle, L., Jacob, D.J., 1998. Airborne in situ OH and HO_2 observations in the cloud-free troposphere and lower stratosphere during SUCCESS. Geophys. Res. Lett. 25, 1701–1705.

Castleman, A.W., Munkelwitz, H.R., Manowitz, B., 1974. Isotopic studies of the sulfur component of the stratospheric aerosol layer. Tellus 26, 222–234.

DeMore, W.B., Sander, S.P., Golden, D.M., Hampson, R.F., Kurylo, M.J., Howard, C.J., Ravishankara, A.R., Kolb, C.E., Molina, M.J., 1997. Chemical kinetics and photochemical data for use in stratospheric modeling, evaluation number 11. JPL Publ. 97–4. NASA Jet Propulsion Laboratory, Pasadena, CA.

Fischer, H., Wienhold, P., Hoor, P., Bujok, O., Schiller, C., Siegmund, P., Ambaum, M., Scheeren, H.A., Lelieveld, J.,

2000. Tracer correlations in the northern high latitude lowermost stratosphere: influence of cross-troposphere mass exchange. Geophys. Res. Lett. 27, 97–100.

Francis, P., Maciejewski, A., Oppenheimer, C., Chaffin, C., Caltabiano, T., 1995. SO_2:HCl ratios in the plumes from Mt. Etna and Vulcano determined by Fourier transform spectroscopy. Geophys. Res. Lett. 22 (13), 1717–1720.

Grainger, R., Highwood, E. (Eds.), Changes in Stratospheric Composition, Chemistry, Radiation and Climate Caused by Volcanic Eruptions. Volcanic Degassing, Geological Society Special Pub., vol. 213. Geological Society, Bath, UK.

Hanisco, T.F., Lanzendorf, E.J., Wennberg, P.O., Perkins, K.K., Stimpfle, R.M., Voss, P.B., Anderson, J.G., Cohen, R.C., Fahey, D.W., Gao, R.S., Hintsa, E.J., Salawitch, R.J., Margitan, J.J., McElroy, C.T., Midwinter, C., 2001. Sources, sinks, and the distribution of OH in the lower stratosphere. J. Phys. Chem., A 105, 1543–1553.

Hipskind, R.S., Gregory, G.L., Sachse, G.W., Hill, G.F., Danielsen, E.F., 1987. Correlations between ozone and carbon monoxide in the lower stratosphere, folded tropopause, and maritime troposphere. J. Geophys. Res. 92, 2121–2130.

Hobbs, P.V., Radke, L.F., Eltgroth, M.W., Hegg, D.A., 1981. Airborne studies of the emissions from the volcanic eruptions of Mount St. Helens. Science 211, 816–818.

Hoor, P., Fischer, H., Lange, L., Lelieveld, J., Brunner, D., 2002. Seasonal variations of a mixing layer in the lowermost stratosphere as identified by the $CO–O_3$ correlation from in-situ measurements. J. Geophys. Res. 107 (D5), ACL1.

Horrocks, L., Burton, M., Francis, P., Oppenheimer, C., 1999. Stable gas plume composition measured by OP-FTIR spectroscopy at Masaya Volcano, Nicaragua, 1998–1999. Geophys. Res. Lett. 26 (23), 3497–3500.

Hunton, D.E., Ballenthin, J.O., Borghetti, J.F., Federico, G.S., Miller, T.M., Thorn, W.F., Viggiano, A.A., Anderson, B.E., Cofer, W.R., McDougal, D.S., Wey, C.C., 2000. Chemical ionization mass spectrometric measurements of SO_2 emissions from jet engines in flight and test chamber operations. J. Geophys. Res. 105 (D22), 26841–26856.

Jonsson, H.H., Wilson, J.C., Brock, C.A., Knollenberg, R.G., Newton, R., Dye, J.E., Baumgardner, D., Borrmann, S., Ferry, G.V., Pueschel, R., Woods, D.C., Pitts, M.C., 1995. Performance of a focused cavity aerosol spectrometer for measurements in the stratosphere of particle size in the 0.06–2.0 micron diameter range. J. Oceanogr. Atmos. Technol. 12, 115–129.

Klein, K., Toon, O.B., Anderson, B., Ballenthin, J.O., Hunton, D.E., Miller, T.M., Viggiano, A.A., 2000. Modeling the conversion of SO_2 to aerosol in the Hekla volcanic plume and comparison with data. AGU Fall Meeting. American Geophysical Union, San Francisco, CA.

Koike, 2000 (private communication).

Krotkov, N.A., Krueger, A.J., Bhartia, P.K., 1997. Ultraviolet optical model of volcanic clouds for remote sensing of ash and sulfur dioxide. J. Geophys. Res. 102 (D18), 21891–21904.

Krueger, A.J., Krotkov, N.A., Lait, L., Burris, J., McGee, T., Twigg, L., Fromm, M.D., Hunton, D.E., Ballenthin, J.O., Miller, T.M., Viggiano, A.A., Anderson, B.E., 2000. The plume from the

February 26, 2000 eruption of Mt. Hekla, Iceland. Spring Meeting Am. Geophys. Un., Baltimore, MD.

Lait, L.R., 2002. Goddard Automailer. GSFC Code 916 Atmospheric Chemistry and Dynamics Branch.

Mankin, W.G., Coffey, M.T., 1984. Increased stratospheric hydrogen chloride in the El Chichón Cloud. Science 226, 170–172.

Mankin, W.G., Coffey, M.T., Goldman, A., 1992. Airborne observations of SO_2, HCl and O_3 in the stratosphereic plume of the Pinatubo volcano in July 1991. Geophys. Res. Lett. 19 (2), 179–182.

Mather, T.A., Allen, A.G., Davison, B.M., Pyle, D.M., Oppenheimer, C., McGonigle, A.J.S., 2004. Nitric acid from volcanoes. Earth Planet. Sci. Lett. 218, 17–30.

Miller, T.M., Ballenthin, J.O., Meads, R.F., Hunton, D.E., Thorn, W.F., Viggiano, A.A., Kondo, Y., Koike, M., Zhao, Y., 2000. CIMS technique for the measurement of HNO_3 in air traffic corridors in the upper troposphere during the SONEX campaign. J. Geophys. Res. 105 (D3), 3701–3707.

Newman, P.A., Harris, N.R.P., Adriani, A., Amanatidis, G.T., Anderson, J.G., Braathen, G.O., Brune, W.H., Carslaw, K.S., Craig, M.S., DeCola, P.L., Guirlet, M., Hipskind, R.S., Kurylo, M.J., Küllmann, H., Larsen, N., Mégie, G.J., Pommereau, J.-P., Poole, L.R., Schoeberl, M.R., Stroh, F., Toon, O.B., Trepte, C.R., Van Roozendael, M., 2002. An overview of the SOLVE/THESEO 2000 campaign. J. Geophys. Res. 107 (D20) (SOL 1-1 to SOL 1-26, 8259, doi:10.1029/2001JD001303).

Oppenheimer, C., Francis, P., Maciejewski, A.J.H., 1998. Spectroscopic observations of HCl degassing from Soufriere Hills volcano, Montserrat. Geophys. Res. Lett. 25 (19), 3689–3692.

Oskarsson, N., 1980. The interaction between volcanic gases and tephra: fluorine adhering to tephra of the 1970 Hekla eruption. J. Volcanol. Geotherm. Res. 8, 251–266.

Oskarsson, N., 1981. The chemistry of Icelandic lava incrustations and the latest stages of degassing. J. Volcanol. Geotherm. Res. 10, 93–111.

Qiu, S., Arnold, F., 1982. Stratospheric in-situ measurements of H_2SO_4 and HSO_3 vapors during a volcanically active period. Planet. Space Sci. 32 (1), 87–95.

Qiu, S., Arnold, F., 1988. Abnormal increase of HNO_3 concentration in the El Chichon volcanic clouds. Kexue Tongbao 33, 591.

Read, W.G., Froidevaux, L., Waters, J.W., 1993. Microwave limb sounder measurements of stratospheric SO_2 from the Mt. Pinatubo Volcano. Geophys. Res. Lett. 20 (12), 1299–1302.

Robock, A., 2000. Volcanic eruptions and climate. Rev. Geophys. 38 (2), 191–219.

Rose, W.I., Gu, Y., Watson, I.M., Yu, T., Bluth, G.J.S., Prata, A.J., Krueger, A.J., Krotkov, N., Carn, S., Fromm, M.D., Hunton, D.E., Ernst, G.G.J., Viggiano, A.A., Miller, T.M., Ballenthin, J.O., Reeves, J.M., Wilson, J.C., Anderson, B.E., Flittner, D.E., 2003. The February–March 2000 eruption of Hekla, Iceland from a satellite perspective. In: Robock, A., Oppenheimer, C. (Eds.), AGU Geophysical Monograph 139 Volcanism and Earth's Atmosphere, pp. 107–132.

Schoeberl, M.R., Sparling, L.C. (Eds.), Trajectory Modelling. Diagnostic Tools in Atmospheric Physics, Proc. S. I. F. Course CXVI. North-Holland, Amsterdam.

Solomon, S., 1999. Stratospheric ozone depletion: a review of concepts and history. Rev. Geophys. 37 (3), 275–316.

Tabazadeh, A., Turco, R.P., 1993. Stratospheric chlorine injection by volcanic eruptions: HCl scavenging and implications for ozone. Science 260, 1082–1086.

Talbot, R.W., Dibb, J.E., Scheuer, E.M., Kondo, Y., Koike, M., Singh, H.B., Salas, L.B., Fukui, Y., Viggiano, A.A., Ballenthin, J.O., Meads, R.F., Miller, T.M., Hunton, D.E., Blake, D.R., Blake, N.J., Atlas, E., Flocke, F., Jacob, D.J., Jaegle, L., 1999.

Reactive nitrogen budget during the NASA SONEX mission. Geophys. Res. Lett. 26 (20), 3057–3060.

Turco, R.P., Whitten, R.C., Toon, O.B., 1982. Stratospheric aerosols: observation and theory. Rev. Geophys. Space Phys. 20, 233.

Viggiano, A.A., Hunton, D.E., 1999. Airborne mass spectrometers: four decades of atmospheric and space research at the air force research laboratory. J. Mass Spectrom. 34, 1107–1129.

Wayne, R.P., 1991. Chemistry of Atmospheres. Clarenden Press, Oxford.